1.1 THE CALIFORNIA LOW-LEVEL COASTAL JET AND NEARSHORE STRATOCUMULUS

John Kalogiros and Qing Wang*
Naval Postgraduate School, Monterey, California

1. INTRODUCTION

This observational study focus on the interaction between the coastal wind field and the evolution of the coastal stratocumulus clouds. The data were collected during an experiment in the summer of 1999 near the California coast with the Twin Otter research aircraft operated by the Center for Interdisciplinary Remote Piloted Aircraft Study (CIRPAS) at the Naval Postgraduate School (NPS). The wind components were measured with a DGPS/radome system, which provides a very accurate (0.1 ms^{-1}) estimate of the wind (Kalogiros and Wang 2001). The instrumentation of the aircraft included fast sensors for the measurement of air temperature, humidity, shortwave and longwave radiation, sea surface temperature, liquid water and concentration and size of water droplets and aerosols.

The synoptic conditions during the experimental period were typical of a high pressure system over the central Pacific Ocean with lower pressure over land and northerly winds in the 2km layer close to the surface. The wind speed was observed to increase in the boundary layer and a wind jet close to the boundary layer top was frequently observed some tens of kilometers offshore. In some occasions the wind jet was quite intense and affected significantly the structure of the stratocumulus layer.

2. THE MARINE BOUNDARY LAYER OF THE CALIFORNIA COAST

Two significant characteristics of the marine boudary layer of the California coast are the stratocumulus clouds and the low-level coastal wind jet. The cold sea surface temperatures near the coast due to upwelling and the strong temperature inversion at the top of the boundary layer due the synoptic scale subsidence favor the development of stratocumulus cloud during the summer. The coastal wind jet is mainly the result of the large horizontal temperature gradient (baroclinity) between the cold air above the sea and the warm air above land (thermal wind) and the frictional effect within the atmospheric boundary layer (Zemba and Friehe 1987, Burk and Thompson 1996). The horizontal temperature gradient follows the orientation of the coastline (317° on the average in central California). Thus, the thermal wind has a northern and an eastern component and local maximum of both components of the wind is expected close to the top of the boundary layer. Topographical features may intensify this wind jet at significant convex bends of the coastline like Cape Mendocino, Pt Arena and Pt Sur. At such changes of the coastline geometry combined with mountain barriers (channeling effect) the northerly flow can become supercritical. An expansion fan occurs at the bend and a strong wind jet evolves downstream of the bend (Winant et al. 1988).

During the experimental period the marine boundary layer top was characterized by a strong temperature inversion of 5-10°C due to the synoptic scale subsidence and its height varied from 400-500 m close to the shoreline to 800 m about 200 km offshore. The cloud top is just below the temperature inversion and cloud top radiative cooling further intensified the temperature inversion. The cloud depth was typically 300m with maximum liquid water content of 0.4-0.6 gkg^{-1} and effective droplet radius 8-10 μm near cloud top. The concentration of droplets varied between 150 and 200 cm^{-3}.

3. INTERACTION OF THE COASTAL JET WITH STRATOCUMULUS

On the flight of 6 of July 1999 a strong wind jet (peak wind speed of 20 ms^{-1}) was observed at the height of 500 m just below the temperature inversion base (boundary layer height) about 75 km offshore (-122.7° longitude). Figure 1 shows contours of the observed wind components in the area of the wind jet. This wind jet seemed to be connected with a zone of cloud breakup parallel to the shore (Fig. 2). As it can be seen in the figure the north edge of the cloud free zone is at Cape Mendocino. During the day this cloud free zone expanded to the south near Pt. Conception.

* *Corresponding author address*: Qing Wang, Naval Postgraduate School, Dept. of Meteorology, Monterey, CA 93943; e-mail: qwang@nps.navy.mil.

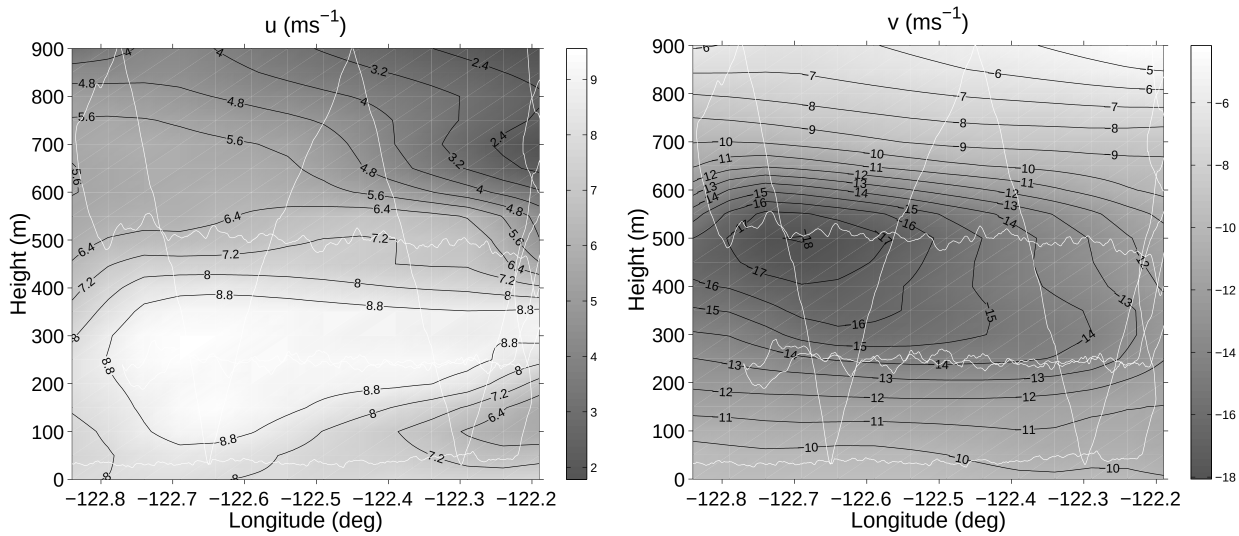

Figure 1. Contours of the observed wind components (u: east, v: north) in the area of the wind jet in the time period 1730 to 1900 UTC. The white line is the track of the aircraft.

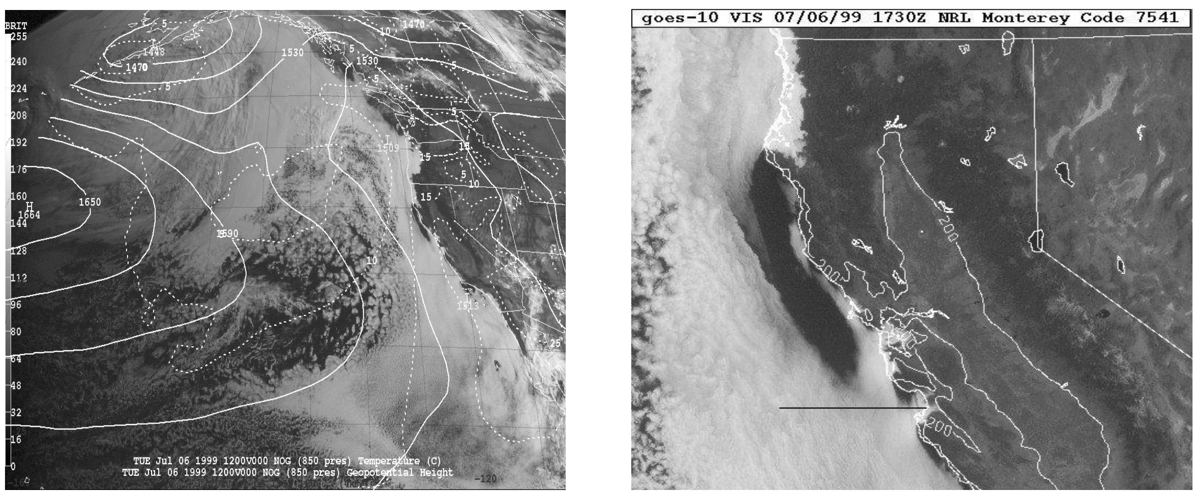

Figure 2. Visible satellite pictures in the area of the experiment. The black line at the bottom of the second picture is the horizontal projection of the approximate path of the aircraft.

Similar cloud free zones, but with less intense characteristics, were observed during other experimental days (19 of June, 8-9 and 16-17 of July). The flight track on the 6th of July reached 250 km offshore keeping almost constant latitude (36.7°N, Monterey bay) which is just at the south edge of the cloud free zone in Fig. 2. Soundings and straight, level legs were performed.

Figure 3 shows the observed cloud base and top with longitude in the time period 1700 to 1900 UTC. The cloud top is coincident with the base of the strong temperature inversion (about 10 K increase in 70 m depth) capping the cloudy marine boundary layer. This height increases almost linearly with distance from the shore. The cloud base on the other hand shows a rapid increase to the west of -122.2° longitude, reaches a maximum at about –122.7° and then decreases again until –123.3°. Thus, it is evident that there is a local thinning of the cloud from a 300m depth to 100m in this area. The straight lines in Fig. 3 are linear fit by eye to the cloud top and the expected cloud base. This was estimated from the lifting condensation level (LCL) using data from a straight level flight leg at 30m above the sea surface. It should be noted that during a flight leg at a height of 425 m passing from –122.7° at about 1600 UTC the cloud base at that longitude was estimated to be at about 350 m assuming adiabatic liquid water. The soundings during two different times at –122.2° in Fig. 4 show the rapid

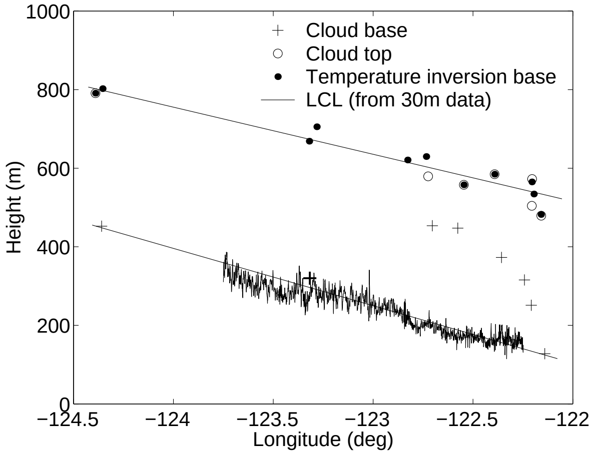

Figure 3. Observed height of temperature inversion base and cloud top and base in the time period 1700 to 1900 UTC.

lift of the cloud base, while the cloud top height changes very little. Figure 5 shows measured air temperature reduced from 30 m to sea surface using the dry adiabatic lapse rate and sea surface temperature. The sea surface temperature shows a general increase with distance from the shore but with significant variations (local minima), which are most possibly cold pools due to local upwelling. Air temperature shows a similar general trend to increase with distance from the shore, but with less variation. However, at -122.7° the air temperature shows a steep drop, which is combined with the local sea surface temperature drop. Figure 5 also shows heat and humidity turbulent fluxes along the same flight leg. The local minima of heat and humidity fluxes correspond to the minima of the difference between sea surface

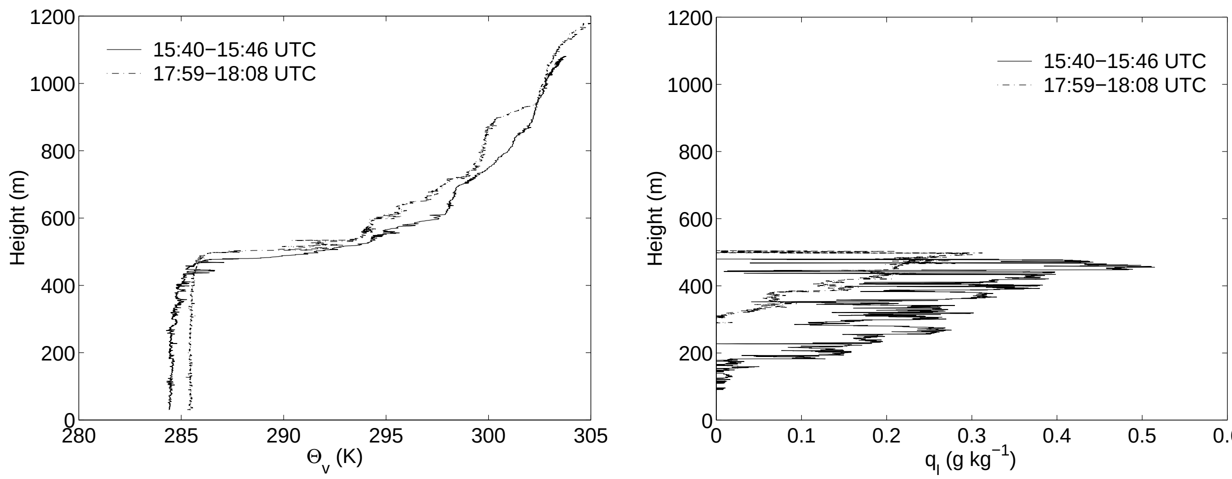

Figure 4. Profiles of virtual potential temperature (Θ_v) and liquid water (q_l) observed near the point with latitude 36.7°N and longitude 122.2°W at the beginning and the end of the flight.

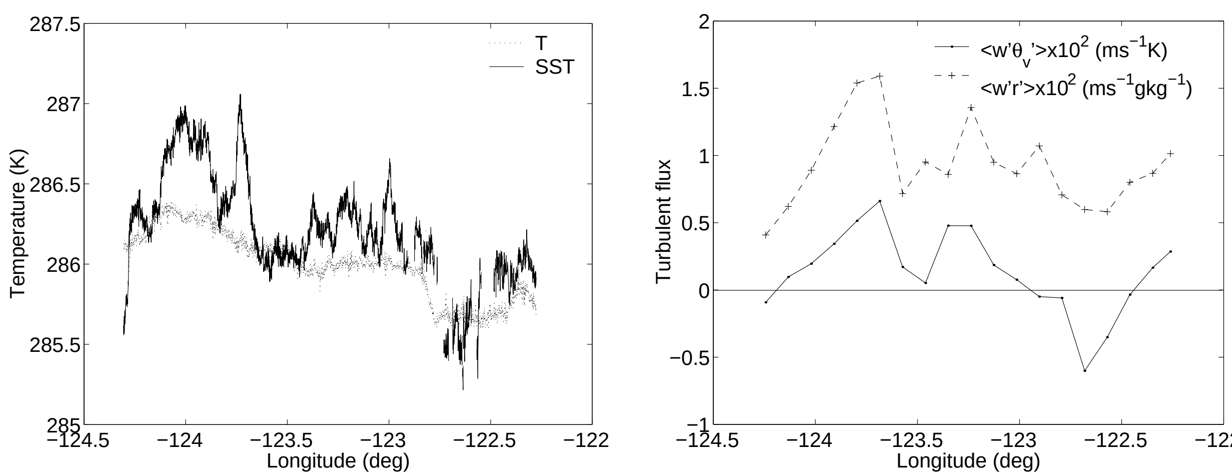

Figure 5. Measured air temperature (T) reduced from 30 m to sea surface using the dry adiabatic lapse rate and sea surface temperature (SST) and heat and humidity turbulent fluxes <w'θ_v'> and <w'r'>, respectively, for the same low-level flight leg as in Figure 3.

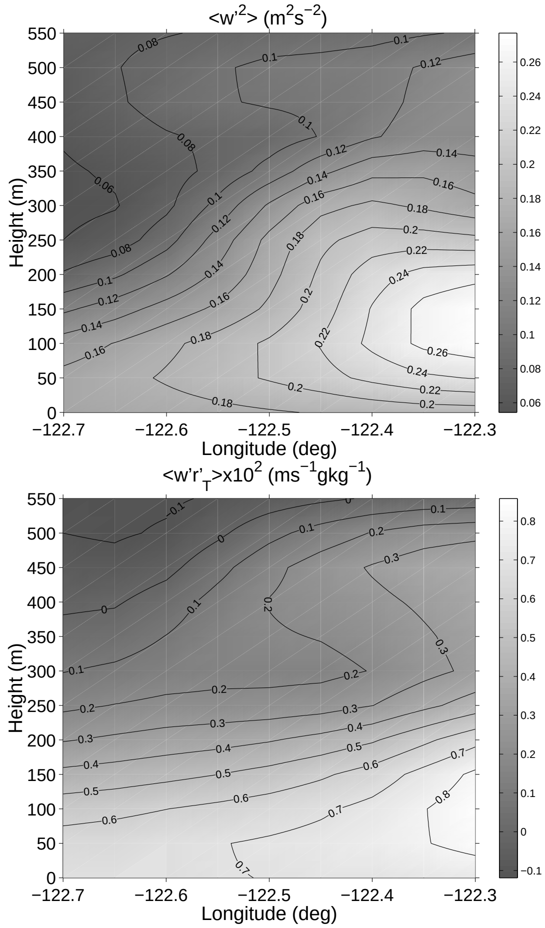

Figure 6. The variance of the vertical wind velocity <w'^{2}> and the turbulent flux of total water <w'r$_T$'> at the area of the wind jet in the time period 1730 to 1900 UTC.

temperature and air temperature as it is expected. The cold sea temperature pool may be the result of local upwelling due to favorable curl of the surface wind stress (Enriquez and Friehe 1995).

Figure 6 shows contours of vertical velocity variance and turbulent flux of total water at the area of the wind jet in the time period 1730 to 1900 UTC. The legs used in the calculation of the turbulent quantities were 10 km long. The total water flux includes also the gravitational settling of droplets estimated using the droplet spectra measured with an FSSP. The total water flux has a minimum near zero at the core of the wind jet. This observation and the negative buoyancy surface flux indicate that the subcloud and cloud layer are decoupled form the surface mixed layer (Nicholls 1984). During the earlier (1600 UTC) flight leg at a height of 425 m and about –122.7° and within the cloud a strong negative buoyancy flux was observed in this area. This may be the result of significant entrainment at the temperature inversion due to wind shear, but the inversion height did not change significantly during the observation time (Fig. 4). The profiles of virtual and equivalent potential temperature at the jet core (not shown here) are also characterized by a stable stratification well below cloud base that prevents the coupling of the cloud with the surface mixed layer. The vertical velocity variance is low just below the jet core, which assists in the decoupling of the cloud layer from the surface.

4. CONCLUSIONS

The strong low-level coastal wind jet is probably the source of the local decoupling of the cloud from the surface layer and its rapid thinning and breakup during the case described here. The decoupling cannot be the result of solar radiation absorption by the cloud alone because it occurred in a limited zone only. The wind jet may affect the local upwelling and, thus, the sea surface temperature leading to negative surface buoyancy flux. This result along with the local minimum of turbulence near the jet core may effectively decouple the cloud layer from the surface.

ACKNOWLEDGEMENTS

The present work was sponsored by the National Science Foundation (NSF) grant ATM9900496.

REFERENCES

Burk, S. D., and W.T. Thompson, 1996: The summertime low-level jet and marine boundary layer structure along the California coast. *Mon. Wea. Rev.*, **124**, 668-686.

Enriquez, A.G., and C.A. Friehe, 1995: Effects of wind stress and wind stress curl variability on coastal upwelling. *J. Phys. Oceanogr.*, **25**, 1651-1671.

Kalogiros, J.A., and Q. Wang, 2001: Calibration of a radome-differential GPS system on a Twin Otter research aircraft for turbulence measurements, *J. Atmos. Oceanic Technol.*

Nicholls, 1984: The dynamics of stratocumuls: aircraft observations and comparisons with a mixed layer model. *Quart. J. R. Met. Soc.*, **110**, 783-820.

Winant, C.D., C.E. Dorman, C.A. Friehe and R.C. Beardsley, 1988: The marine layer off the northern California: An example of supercritical flow. *J. Atmos. Sci.*, **45**, 3588-3605.

Zemba, J., and C.A. Friehe, 1987: The marine atmospheric boundary layer jet in the Coastal Ocean Dynamics Experiment. *J. Geophys. Res.*, **92** (C2), 1489-1496.